Peer-reviewed version available at *Viruses* **2019**, *12*, 12; doi:10.3390/v12010012

Article

The Zebrafish Xenograft Platform – A Novel Tool for Modeling KSHV-Associated Diseases

Eric S. Pringle[1, 2, †], Jaime Wertman[1, †], Nicole Melong[3], Andrew J. Coombs[4], Andrew L. Young[5], David O'Leary[5], Chansey Veinotte[1], Carolyn-Ann Robinson[1], Michael N. Ha[6], Graham Dellaire[2, 7], Todd Druley[5], Craig McCormick[1, 2, *], Jason N. Berman[1, 3, 4, *]

[1] Department of Microbiology & Immunology, Dalhousie University, 5850 College Street, Halifax, NS B3H 4R2, Canada
[2] Beatrice Hunter Cancer Research Institute; 5850 College Street, Halifax, NS B3H 4R2, Canada
[3] CHEO Research Institute/Department of Pediatrics, University of Ottawa, Ottawa, ON K1H 8L1, Canada
[4] Department of Pediatrics, Dalhousie University, 5980 University Ave, Halifax, NS B3K 6R8 Canada
[5] Division of Hematology and Oncology, Department of Pediatrics, Washington University School of Medicine, USA
[6] Department of Radiation Oncology, 5820 University Ave, Halifax, NS B3H 1V7, Canada
[7] Department of Pathology, Dalhousie University; 5850 College Street, Halifax, NS B3H 4R2, Canada

[†] These authors contributed equally to this work
* Correspondence: craig.mccormick@dal.ca (C.M.); jberman@cheo.on.ca (J.N.B.)

Abstract: Kaposi's sarcoma associated-herpesvirus (KSHV, also known as human herpesvirus-8) is a gammaherpesvirus that establishes life-long infection in human B lymphocytes. KSHV infection is typically asymptomatic but immunosuppression can predispose KSHV-infected individuals to primary effusion lymphoma (PEL); a malignancy driven by aberrant proliferation of latently infected B lymphocytes, and supported by pro-inflammatory cytokines and angiogenic factors produced by cells that succumb to lytic viral replication. Here, we report the development of the first *in vivo* model for a virally-induced lymphoma in zebrafish, whereby KSHV-infected PEL tumour cells engraft and proliferate in the yolk sac of zebrafish larvae. Using a PEL cell line engineered to produce the viral lytic switch protein RTA in the presence of doxycycline, we demonstrate drug-inducible reactivation from KSHV latency *in vivo*, which enabled real-time observation and evaluation of latent and lytic phases of KSHV infection. In addition, we developed a sensitive droplet digital PCR method to monitor latent and lytic viral gene expression and host cell gene expression in xenografts. The zebrafish yolk sac is not well-vascularized and using fluorogenic assays we confirmed that this site provides a hypoxic environment that may mimic the microenvironment of some human tumors. We found that PEL cell proliferation in xenografts was dependent on the host hypoxia-dependent translation initiation factor, eukaryotic initiation factor 4E2 (eIF4E2). This demonstrates that the zebrafish yolk sac is a functionally hypoxic environment and xenografted cells must switch to dedicated hypoxic gene expression machinery to survive and proliferate. The establishment of the PEL xenograft model enables future studies that exploit the innate advantages of the zebrafish as a model for genetic and pharmacologic screens.

Keywords: Kaposi's sarcoma-associated herpesvirus (KSHV); human herpesvirus-8; zebrafish; ddPCR; xenotransplantation; primary effusion lymphoma (PEL); hypoxia

1. Introduction

Kaposi's sarcoma-associated herpesvirus (KSHV, also known as human herpesvirus-8, or HHV8) is the infectious cause of Kaposi's sarcoma (KS), primary effusion lymphoma (PEL) and multicentric Castleman's Disease (MCD) [1]. KSHV is a gammaherpesvirus that achieves life-long infection of human hosts by establishing latency in immature B lymphocytes and promoting differentiation into a plasmablast-like cell type [2]. An essential feature of herpesvirus latency is reversibility, and periodic reactivation from latency enables lytic KSHV replication to infect new hosts. Accordingly, KSHV latency is unstable *in vivo* and *in vitro*, with spontaneous expression of lytic antigens [3]. PEL is a rare disease that occurs most frequently in human immunodeficiency virus (HIV)-positive individuals, or otherwise immunosuppressed individuals. PEL prevalence remains unclear, but a single 15-year institution study concluded that PEL accounts for approximately 4% of non-Hodgkin's lymphomas (NHLs) [4]. PEL develops as bloody effusions in body cavities, including pleural, peritoneal, and pericardial spaces, but can also form solid extracavity lymphomas [5]. Survival is poor and the rarity of the disease has contributed to a dearth of clinical trials evaluating the most effective treatments. The current standard of care is EPOCH (Etoposide, Prednisone, Oncovin/vincristine, Cyclophosphamide, Hydroxydaunorubicin/doxorubicin) or CHOP with or without antiretroviral therapy [5].

Patient-derived PEL cell lines can be grown in culture and retain the KSHV episome as a latent infection. While readily amenable to experimentation, these *in vitro* cultures do not fully recapitulate all features of the cancer; thus, providing motivation for the development of *in vivo* PEL models. PEL cell lines readily engraft and proliferate in the abdominal cavity of severe-combined immunodeficiency (SCID) mice, or form subcutaneous solid tumors when injected with Matrigel; the latter of which mimics some aspects of the tumour microenvironment by providing an extracellular matrix [6]. In mice, PEL xenografts regress with rapamycin treatment [7], as they do in KS [8], due to the loss of mTORC1-dependent paracrine and autocrine cytokine signaling required for PEL proliferation [7]. This reliance on paracrine and autocrine signals provides ample rationale for further development of *in vivo* PEL models that afford opportunities to evaluate the influence of the tumor microenvironment.

Zebrafish larvae have emerged as a robust and efficient *in vivo* model for human tumor xenotransplantation (XT), especially human lymphomas and leukemias [9]. Zebrafish share remarkable genetic similarity with humans and have several advantages as a low-cost experimental model, including high fecundity and rapid development. Zebrafish larvae are optically transparent and lack an adaptive immune system until 28 days post-fertilization [10], making them an attractive animal XT model with no requirement for immunosuppression. Furthermore, the zebrafish XT platform allows for the rapid and direct observation and imaging of tumor cell dynamics in a live animal microenvironment in real-time. Particularly important for blood cancers, the developmental process of hematopoiesis is highly conserved in zebrafish, making it an excellent model to study normal and abnormal blood development and disorders [11]. Previously, we successfully transplanted and measured proliferation and migration of leukemia cell lines and primary leukemic cells in zebrafish embryos [12,13] . This zebrafish patient-derived xenograft (PDX) platform enables rapid evaluation of patient tumor cell response to several anti-cancer drugs. For example, xenografts from a patient with T-cell acute lymphoblastic leukemia (ALL) harboring a previously uncharacterized *NOTCH1* mutation (A1696D), were specifically susceptible to a gamma secretase inhibitor [13]. The success of the zebrafish XT platform for studies using leukemia cells suggests that zebrafish larvae might provide a suitable host environment for PEL and could be utilized for further preclinical drug studies or potentially facilitate rapid patient-derived xenotransplation to inform personalized treatment decisions.

Here we successfully engraft and observe the proliferation of a KSHV-infected PEL cell line and KSHV infected epithelial cells in zebrafish larvae. We demonstrate that tetracycline (Tet)-inducible

gene expression is feasible in the zebrafish XT context, although it was inefficient at reactivating KSHV from latency. We further demonstrate the sensitivity and specificity of droplet digital PCR (ddPCR) to selectively measure the expression of human and viral genes in xenografted larvae. To assess oxygen levels in the zebrafish larvae, we used a hypoxia-sensitive dye to label the cells, and confirmed that the yolk sac is a low-oxygen environment. To further explore the effects of the hypoxic microenvironment in the larvae, we silenced expression of eIF4E2, the essential cap-binding protein of hypoxia-specific translation initiation machinery, and demonstrated its requirement for PEL proliferation in the yolk sac. Like other hematological cancers, we demonstrate for the first time that viral lymphomas can proliferate in the zebrafish yolk sac. Thus, future drug discovery studies aimed at treatments for PEL and other viral lymphomas could similarly benefit from further "*in-Danio*" xenotransplantation approaches.

2. Materials and Methods

2.1 Ethics statement and zebrafish husbandry

Adult *casper* [14] zebrafish were maintained in a recirculating commercial housing system (Pentair, Apopka, FL) at 28°C in 14 h:10 h light:dark conditions and bred according to standard protocol [15]. Embryos were collected and grown in E3 medium (5 mM NaCl, 0.17 mM KCl, 0.33 mM $CaCl_2$, 0.33 mM $MgSO_4$) in 10 cm Petri plates at 28°C. Embryos were cleaned and provided with new media every 24 h and used experimentally before 7 days post-fertilization (dpf). Zebrafish embryos (0-72 hours post-fertilization) are considered to enter the larval stage after 3 days post-fertilization (dpf). The use of zebrafish in this study was approved by and conducted in accordance with the policies of the Dalhousie University Committee on Laboratory Animals under protocols #17-131 and #17-055.

2.2 Cell lines

Body-cavity-based lymphoma (BCBL1) cells are a clone derived by limiting dilution of patient derived PEL cells [16]. TREx-BCBL1-RTA cells are subclone of BCBL-1 engineered to express the KSHV immediate early gene *RTA* under the control of a tetracycline promoter [17]. Both cell lines were cultured in suspension with RPMI-1640 supplemented with 10% v/v fetal bovine serum (FBS) (GIBCO), 100 IU penicillin and streptomycin (Invitrogen), and 55 μM beta-mercaptoethanol (GIBCO). iSLK.219 cells are a subclone of a Caki-1 derived epithelial cell line engineered to express RTA under a tetracycline promoter [18]. iSLK.219 cells were latently infected with the recombinant KSHV, rKSHV.219 [19]. iSLK.219 cells and 293T cells used for lentivirus generation were maintained in DMEM supplemented with 10% v/v FBS and 100 IU penicillin and streptomycin (Invitrogen). rKSHV.219 contains a puromycin resistance cassette and retention of the viral episome in culture required supplementing the media with 10 μg/mL of puromycin (ThermoFisher) [20]. All cells were maintained at 37°C with 5% CO_2 atmosphere. For *in vitro* growth curves, cells were washed with 1x PBS, then seeded at $2.5x10^5$ cells/mL. Live cells were counted using Trypan Blue (ThermoFisher) and a hemocytometer. To enumerate red fluorescent protein (RFP)+ iSLK.219 cells, cells were fixed with 4% paraformaldehyde for 15 min at room temperature and nuclei were stained with Hoechst 33342 (Invitrogen). Fluorescent images were captured using an EVOS FL Cell Imaging system (ThermoFisher) and RFP+ and Hoeschst+ cells were counted using a custom CellProfiler ver 3.0.0 script [21].

2.3 Zebrafish xenotransplantation

Approximately $5x10^6$ BCBL or TREx-BCBL1-RTA cells were harvested and centrifuged at 1000 x *g* for 5 min. Approximately $2x10^6$ iSLK.219 cells were first dissociated from tissue culture dishes with trypsin and recovered in full media before pelleting. Cell pellets were resuspended with 10 mL of

phosphate-buffered saline (PBS) and 5 μg/mL of CellTracker Orange CMTMR Dye (ThermoFisher). The cells were incubated at 37°C for 20 min then collected by centrifugation. Cells were washed twice with 10 mL full cell culture medium and once with 10 mL PBS. Cells were resuspended to a final volume of approximately 100-150 μL in culture medium for injection. CMTMR Dye was omitted on xenografting of iSLK.219 cells to test *in vivo* reactivation. To test for oxygen concentration in the yolk sac, TREx-BCBL1-RTA cells were incubated with 5 μM of Image-iT Green Hypoxia Reagent (Invitrogen) for 30 min at 37°C. Cells were washed once with PBS after labelling.

Zebrafish embryos were allowed to naturally shed their chorion at 2 dpf. Before injection, embryos were anesthetized with 0.09 mg/mL tricaine solution (Sigma-Aldrich) and arrayed on an agarose plate for cell transplantation as described previously [12]. Experimental cells were loaded into a pulled-glass capillary needle and allowed to settle in the bore of the needle. The needle was then attached to a PLI-100A Pico-Liter microinjection system (Harvard Apparatus, Holliston, MA, USA) and yolk sacs were manually injected with approximately 50-100 cells. The following day, a fluorescent Discovery V20 stereomicroscope (Zeiss, North York, ON, Canada) was used to screen for larvae with an obvious bolus of fluorescent cells in the yolk sac. Following injections, larvae were kept at 35°C for the remainder of the experiment, an established midpoint between the optimal temperature for zebrafish development (28°C) and human cell growth (37°C) [12].

2.4 Zebrafish xenotransplant ex-vivo cell proliferation assay

Positive larvae (those with a compact bolus of cells present in the yolk sac) were separated into appropriate experimental groups of 30-40 and monitored daily in 60 x 15 mm plates at 35°C. For XT cell proliferation data, cells were quantified *ex vivo* at 24 hours post-injection (hpi) (baseline) and 72 hpi (experimental endpoint) (**Figure 1A**). Twenty larvae were euthanized by tricaine overdose (1 mg/mL) and dissociated in collagenase (Sigma-Aldrich) for 30 min. Once dissociated into a single cell suspension, 200 μL of FBS was added to the sample to slow the enzymatic reaction prior to collagenase removal. The sample was then centrifuged at 300 x *g* for 5 min, the supernatant was removed, and the sample was washed once with a 30% v/v FBS in PBS solution and centrifuged once more. The supernatant was removed, leaving the fluorescently labeled human tumor cells among the zebrafish cells. The sample was resuspended in 10 μL/larva solution of 30% v/v FBS in PBS for imaging. Ten 10 μL boli were pipetted onto a "PTFE" Printed glass slide 5 mm well diameter (Electron Microscopy Sciences) and allowed to settle for 8-10 min. The boli were individually imaged using an inverted Axio Observer Z1 microscope (Carl Zeiss) and images were analyzed using ImageJ software (NIH), as in previously published methods [12]. Cell numbers for each experimental group were normalized to baseline cell counts to ensure cells were engrafting and proliferating in the XT model. Experiments were conducted in triplicate for each cell line. Any remaining larvae were euthanized with tricane overdose prior to 7 dpf.

2.5 Zebrafish toxicity experiments

To determine an appropriate doxycycline treatment dose for zebrafish larvae, toxicity assays were conducted to obtain half the maximum tolerated dose (MTD_{50}) [12]. *casper* larvae [14] staged at 72 hours post-fertilization (hpf) were arrayed in 96-well plates and treated with increasing doses of drug for a total of 72 h to ascertain toxicities. Treatment doses for experiments were chosen by halving the dose when 80% larval survival was observed. Toxicity assays were repeated in triplicate.

2.6 Western blotting

TREx-BCBL1-RTA cells were harvested by centrifugation at 1,500 x *g* for 5 min, washing once with ice-cold PBS, pelleting again, then lysing in 2x Laemmli buffer (4% w/v sodium dodecyl sulfate (SDS), 20% v/v glycerol, 120 mM Tris-HCl pH 6.8). Samples were reduced with 100 mM dithiothreitol (DTT) and boiled at 95°C for 5 min. An aliquot of the lysate before reduction and boiling was used to

determine the protein concentration using the DC Protein-Assay (Bio-Rad). Concentrations were normalized and 10 µg of total protein content was analysed by SDS-PAGE and transferred to PVDF membranes using a semi-dry transfer (Trans-Blot Turbo Transfer System and RTA PVDF kit, Bio-Rad). Membranes were blocked with 5% w/v BSA TBS-T, then probed overnight with the following antibodies: myc (Cell Signaling Technologies (CST) #2276); ORF57 (Santa Cruz Biotechnologies sc135746); ORF65 (a kind gift from Jae Jung); β-actin (CST #5125); eIF4E2 (GeneTex GTX103977); and eIF4E1 (CST #2067). Primary antibody binding was detected with horseradish-peroxidase conjugated secondary antibodies (anti-mouse: CST #7076; anti-rabbit #7074). Blots were developed with Clarity–ECL chemiluminescence reagent (Bio-Rad) and imaged on a Chemidoc-Touch (Bio-Rad).

2.7 RT-qPCR analysis

RNA was harvested from TREx-BCBL1-RTA cells using RNeasy (Qiagen) according to the manufacturer's directions. Cells were harvestd by centrifugation at 1,500 x g for 5 min and lysed in RLT buffer from the RNeasy kit. cDNA was generated using Maxima H Minus First Strand Reverse Transcriptase (Thermo Fisher) with random oligo priming and qPCR performed using GoTaq (Promega) on a CFX Connect Realtime PCR system (Bio-Rad) using the following primers (5′-3′): *ORF45* (Forward (F): TGA TGA AAT CGA GTG GGC GG, Reverse (R): CTT AAG CCG CAA AGC AGT GG), *K8.1* (F: AGA TAC GTC TGC CTC TGG GT, R: AAA GTC ACG TGG GAG GTC AC), *β-actin* (F: CTT CCA GCA GAT GTG GAT CA, R: AAA GCC ATG CCA ATC TCA TC), RTA (F: GAT TAC TGC GAC AAC GGT GC, R: TCT GCG ACA AAA CAT GCA GC), *18S* rRNA (F: TTC GAA CGT CTG CCC TAT CAA, R: GAT GTG GTA GCC GTT TCT CAG G). An annealing temperature of 60°C was used for all primers pairs. The abundance of a transcript $\boldsymbol{x}$ was normalized to *18S* rRNA abundance using the formula:

$$\text{Abundance}=2^{(-\Delta Cq)}$$

where:

$$\Delta Cq=Cq_{\boldsymbol{x}}-Cq_{18S}$$

and Cq is the quantitative cycle, as determined automatically by the CFX Manager software (Bio-Rad).

2.8 RNA extraction and digital droplet PCR (ddPCR).

Twenty XT larvae were euthanized and transferred to a 1.5 mL microcentrifuge tube. Water was carefully removed and larvae were subsequently lysed in Buffer RLT (Qiagen RNeasy Plus kit) supplemented with 40 mM of DTT. The larvae were homogenized by repeated passage through a 22-gauge needle (at least 20 times). Subsequent precipitation and isolation of RNA was conducted according to the manufacturer's recommended protocol, including an on column DNAse digestion (Qiagen) Eluted RNA was quantified by nanospectrophotometry (Nanovue GE) and concentrations were equalized prior to reverse transcription with Maxima H (ThermoFisher) with random oligo priming as described above. The resulting cDNA solution was then diluted 1:10 for subsequent ddPCR analysis on the Bio-Rad QX200 ddPCR platform. 20 µL reaction mixtures were assembled using 2X QX200 ddPCR EvaGreen supermix (Bio-Rad), 5 µL of diluted cDNA, and 200 nM of each forward and reverse primer (same primers sequences as described above for qRT-PCR analysis). We included both a RT negative control for cDNA generation and no template controls during PCR to exclude genomic DNA or carryover amplicon contamination. Droplets were generated and PCR was conducted according to the manufacturer's instructions using a 60°C annealing temperature. Fluorescent intensity of droplets were analyzed using QuantaSoft software (Bio-Rad).

2.9 Lentivirus generation

eIF4E2 expression was knocked down using pGIPZ shRNA-expressing lentivirus (ThermoFisher clone V2LHS_68041) or a non-targeting control (clone RHS_4346). Lentiviruses were generated by co-transfecting pGIPZ with psPAX2 and pMD2.G packaging plasmids (kind gifts from Didier Trono Addgene #12259, #12260) in HEK293T cells with polyethylenimine MAX (Polysciences, #24765). Two days after transfection, virus-containing cell supernatants were harvested and cleared with a 0.45 μm filter. Virions were aliquoted and stored at -80°C prior to transduction. We transduced suspension cells by diluting the suspension culture in an equal proportion with lentivirus stock in the presence of 4 μg/mL of polybrene (hexadimethrine bromide, Sigma) and incubating for 24 h. The inoculum was then removed by centrifugation and cells were cultured for several days in the presence of 1 μg/mL puromycin (ThermoFisher) until a consistently GFP+ and puromycin resistant culture was obtained.

2.10 Statistics and data processing

Numerical data was collected and organized in Excel (Microsoft) and histograms were generated in Prism (GraphPad). All statistical tests were calculatd in Prism: * = $p<0.05$, ** = $p<0.01$, ns= non-significant. Error bars are standard error measurement (SEM).

3. Results

3.1 KSHV-infected PEL cells successfully engraft in zebrafish embryos

To determine whether KSHV latently-infected lymphoma cells can successfully engraft in zebrafish we labelled BCBL1 cells, or the TREx-BCBL1-RTA subclone with Tet-regulated reactivation, with the cell permeable dye CMTMR, and microinjected them into the yolk sac of 48 h post-fertilization (hpf) zebrafish embryos. The dye remains incorporated in cells over multiple cycles of cell division, with the signal diminishing proportionally after each division. The following day, these larvae were visually screened for boli of fluorescent cells in the yolk sac and groups of fish were dissociated every day for three days after initial screening (**Figure 1A).** The cells appeared to remain in the yolk sac and we did not detect evidence of migration of tumor cells into surrounding tissues **(Figure 1B)**. Both BCBL1 cells and TREx-BCBL1-RTA cells successfully proliferated in the yolk sac, with BCBL1 cells increasing in number by 2.2-fold and TREx-BCBL1-RTA cells increasing by 2.8 fold over three days (**Figure 1C**). We also monitored the impact of the injection process itself on larval survival. Embryos were either injected at 2 dpf with cells labelled with CMTMR, or were "mock-injected," where sterile cell culture media was injected into the yolk sack. Mock-injected larvae had a slight yet significant decrease in survival compared to uninjected controls after 5 days post-injection (i.e. 7 dpf). Xenografted larvae had significantly poorer survival at 7 dpf compared to mock-injected controls **(Figure 1D).** These data indicate that PEL cells can successfully proliferate in the yolk sac and that the larvae can tolerate xenotransplantation; although the microinjection process diminishes long-term viability of the larvae.

Preprints (www.preprints.org) | NOT PEER-REVIEWED | Posted: 8 November 2019 doi:10.20944/preprints201911.0081.v1

Peer-reviewed version available at Viruses 2019, 12, 12; doi:10.3390/v12010012

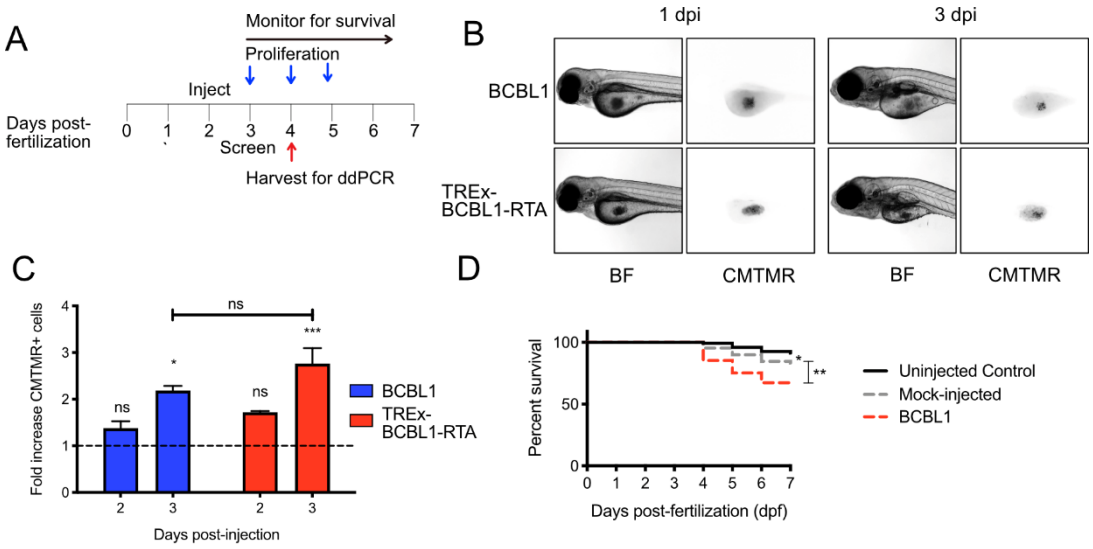

Figure 1. Proliferation of BCBL and TREx-BCBL1-RTA in zebrafish larvae: **(A)** Timeline of xenotransplantation experiment. Fish are xenotransplanted with fluorescent CMTMR-labelled, primary effusion lymphoma cells by microinjection at 2 days post-fertilization (dpf). The following day embryos are visually screened with a fluorescent microscope for viability and the presence of a cell bolus in the yolk sac, as seen in (B). Groups of larvae are sacrificed at indicated times for dissociation and counting of xenotransplanted cells or RNA harvest. Survival of the larvae is monitored throughout the experiment; **(B)** Photomicrographs of xenotransplanted larva demonstrating the bolus of cells in the yolk sac at 1 and 3 days post-injection (dpi), which are 3 and 5 dpf, respectively; **(C)** Proliferation of BCBL1 and TREx-BCBL1-RTA cells at 2 and 3 dpi normalized to the number of cells counted at 1 dpi (n=3 independent experiments with cells from 20 larvae counted per measurement; means ± SEM; statistical significance was determined by two-way ANOVA compared to the cell counts at 1 dpf); **(D)** CMTMR-labelled BCBL1 cells are injected into 2 dpf embryos, which were screened at 3 dpi then survival was monitored until 7 dpf. Uninjected and media mock-injected embryos were included as controls. (n=150 larvae per group accrued from 3 separate hatchings; statistical significance was determined by Mantel-Cox test).

3.2 KSHV-infected epithelial cells successfully engraft and can be induced for lytic replication

KSHV establishes a latent infection in most epithelial cell lines, and all PEL cell lines are latently infected with KSHV [22]. Reactivation from latency requires expression of the immediate early gene *regulator of transcriptional activation (RTA)* that initiates an ordered cascade of gene expression to subvert the host, replicate the viral genome, and package genomes into virions. iSLK.219 cells can be stimulated to induce lytic replication through Tet-driven expression of RTA. We wanted to determine if we could stimulate viral gene expression in zebrafish xenografts by adding doxycycline directly to the embryo water. We pursued these experiments using iSLK.219 cells that are latently infected with the rKSHV.219 virus. These cells constitutively express green fluorescent protein (GFP) from a EF-1α promoter on the viral episome. When viral gene expression is stimulated, a reporter red fluorescent protein (RFP) driven by a viral early promoter PAN is activated, which allows for visual determination of reactivation (**Figure 2A**) [19]. We first tested whether these KSHV-infected epithelial cells would proliferate within the yolk sac. We injected 2 dpf casper embryos with iSLK.219 cells, and similar to what was found with BCBL cells, iSLK.219 cells readily proliferate within the larval yolk sac (**Figure 2B**). The bright GFP fluorescence of the iSLK.219 cells allowed for clear detection of the cell bolus despite the high fluorescent background of the embryos using standard GFP filter sets (500-

550 nm). This allowed us to omit the CMTMR Dye in reactivation experiments and detect reactivated, RFP+ cells.

In cell culture, iSLK.219 cells maintain a tight control of latency and few RFP+ cells can be detected [20]. Addition of doxycycline stimulates the immediate early RTA transgene and within 24 h RFP+ cells can be detected in culture, the proportion of which increases over time **(Figure 2C)**. We attempted to reactivate iSLK.219 cells *in vivo* by adding doxycycline directly to the water in which the larvae were immersed. We tested the toxicity of a range of doxycycline concentrations (0-180 μM) and found that ~80% of fish could tolerate a dose of 100 μM. We then used 40 μg/mL of doxycycline for our fish treatment. One day after injection, 3 dpf embryos containing a GFP+ cell bolus were isolated and treated with 40 μg/mL doxycycline, which was refreshed daily. Similar to what we observed in cell culture **(Figure 2C)** we were unable to detect RFP+ cells in xenotransplanted iSLK.219 even after four days in the yolk sac **(Figure 2D)**. In the doxycycline treated fish we could observe some RFP+ cells after three days of treatment (6 dpf). However, this process was inefficient and we could only observe RFP+ cells in ~20% of the larvae, and very few cells within each larvae were detectably RFP+ **(Figure 2D)**. While inefficient, this suggests that it is possible to activate a Tet-responsive promoter in xenotransplanted cells in the yolk sac and potentially stimulate viral gene expression *in vivo*.

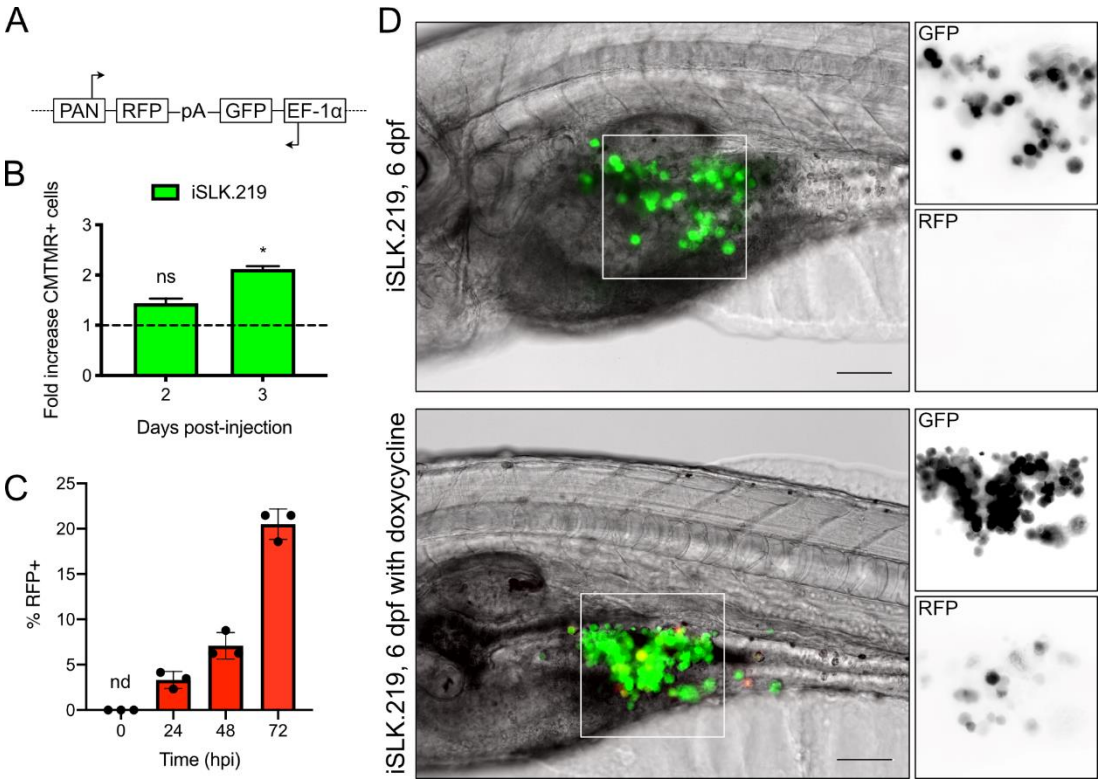

Figure 2. Proliferation and lytic reactivation of iSLK.219 in zebrafish embryos: **(A)** Simplified diagram of rKSHV.219 reporter construct, adapted from [19]. Latently infected cells express GFP from a constitutive EF-1α promoter. During lytic replication, the immediate early protein RTA binds to the viral PAN promoter and stimulates RFP expression. A polyA (pA) signal sequence is present on both strands of the viral genome; **(B)** Proliferation of iSLK.219 cells at 2 and 3 dpi normalized to the number of cells counted at 1 dpi (n= 3 independent experiments with cells from 20 larvae counted per measurement; means ± SEM; statistical significance was determined by two-way ANOVA compared to the cell counts at 1 dpf); **(C)** iSLK.219 cells were treated with 1 μg/mL doxycycline and fixed at the times indicated or

left untreated (Time = 0 hpi). Cells were fixed with 4% paraformaldehyde and nuclei were stained with Hoescht. RFP+ cells and nuclei were imaged on an inverted fluorescent microscope and enumerated with CellProfiler (n=3 independent experiments ± SD, nd = not detected). **(D)** iSLK.219 were injected into the yolk sac of 2 dpf zebrafish embryos. The following days, larvae were screened for viability and a GFP+ cell bolus by fluorescent microscopy. In half the larvae, the E3 media was then supplemented with 40 μg/mL doxycycline, which was refreshed daily. Xenotransplanted larvae were monitored daily for RFP+ cells. Presented here are representative images of both doxycycline-activated and nontreated larvae at the ethical endpoint of the experiment. We could observe RFP+ cells in the yolk sac of approximately 20% of larvae treated with doxycycline, and none in untreated larvae (Scale bar = 100 μm).

3.3 Droplet digital PCR (ddPCR) can detect human and viral transcripts in a PEL xenograft.

Monitoring xenografted cells in the zebrafish typically relies on prior fluorescent labeling of the cells. In this study and in others, our group has employed fluorescence or human antibody immunohistochemistry-based *ex vivo* quantification to enumerate xenografted cells at various time points [12]. Techniques to measure changes in gene expression in human xenografts have been hindered by the paucity of human transcripts in the background of zebrafish RNA. In this study we took advantage of the sensitivity and specificity of droplet digital PCR (ddPCR) to measure changes in gene expression in our xenografts [23]. In ddPCR, the PCR solution is emulsified into droplet suspension to partition the cDNA into positive or negative reactions that are recorded through a microfluidic fluorescence detector.

The full KSHV lytic gene expression program is initiated by the immediate-early gene product RTA, which stimulates expression of early genes that subvert the host cell, counter innate immune defences, and initiate viral genome replication. Late gene expression follows viral genome replication and generates structural proteins required for virion assembly and genome packaging. Like the iSLK.219 cells, TREx-BCBL1-RTA cells express RTA under a Tet-inducible promoter [17]. Doxycycline treatment reactivates the virus from latency; early gene expression (e.g. ORF45) can be detected after 24 h and late gene expression (e.g. K8.1) can be readily detected by 48 h post-reactivation. Late gene expression is dependent on genome replication, which can be prevented using phosphonoacetic acid (PAA), a herpesvirus DNA-dependent DNA-polymerase inhibitor [24] **(Figure 3A-B)**.

Due to the inefficiency of stimulating reactivation from latency in xenotransplanted iSLK.219 cells, we instead pre-treated the TREx-BCBL1-RTA cells for 12 h with doxycycline to initiate virus replication prior to injection into the yolk sac to ensure viral reactivation, then harvested total RNA from the xenotransplanted larvae at 2 dpi (**Figure 3C**). We were able to detect human *β-actin* (*ACTB*) transcripts in the injected larvae but not in our mock-injected controls, demonstrating that is it possible to detect human mRNAs from a limited number of xenotransplanted cells against the background of far more abundant zebrafish transcripts. We were also able to detect the KSHV immediate early transcript *RTA*, the early transcript *ORF45*, and the late transcript *K8.1* in doxycycline-treated xenotransplanted cells. We can also detect *RTA* and *ORF45* in cells that were not treated with doxycycline, likely representing spontaneous entry into lytic replication. The presence of *K8.1* in the xenografted cells suggests that the larval yolk sac microenvironment does not inhibit progression through lytic replication and viral genome replication.

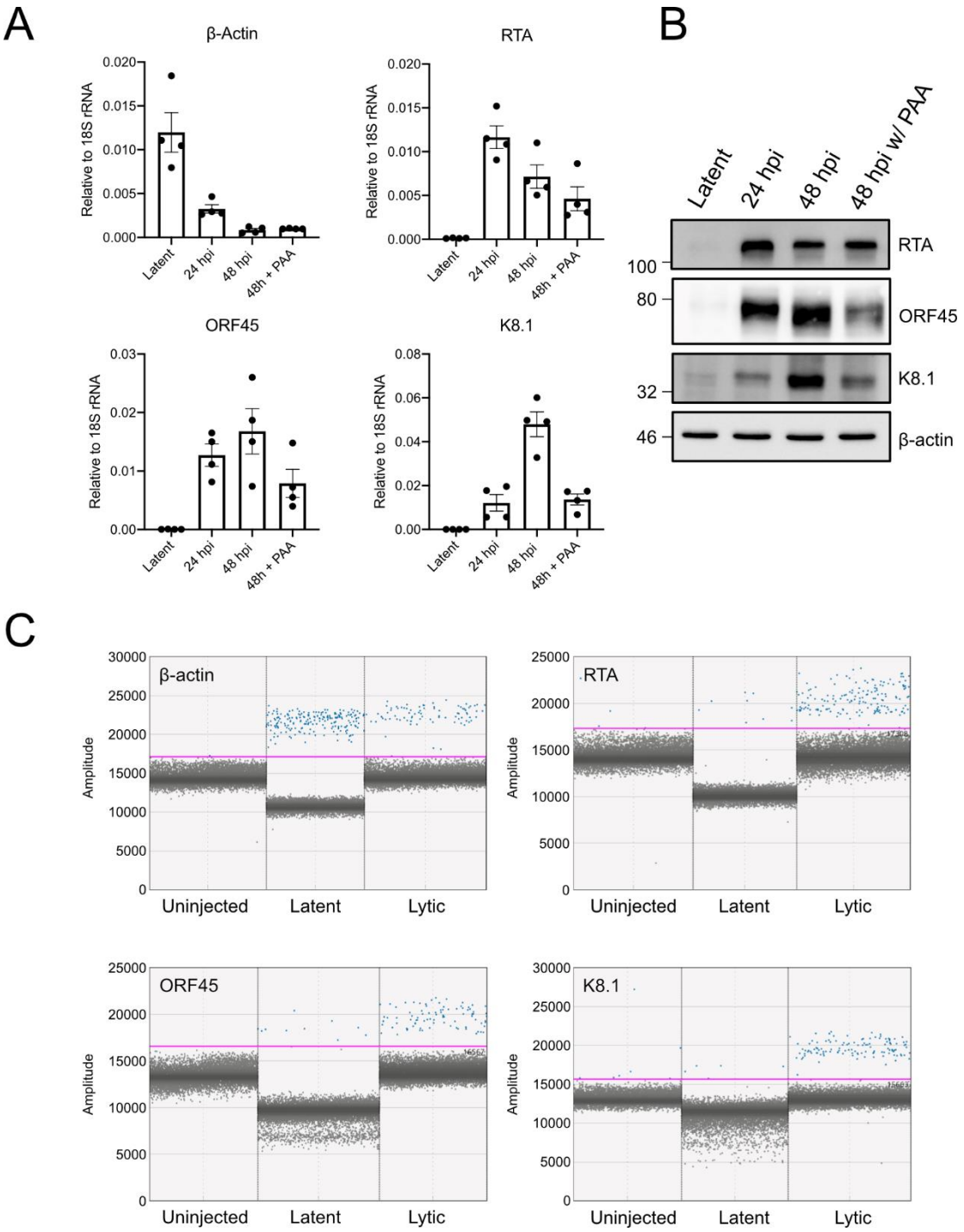

Figure 3. Detection of viral gene expression in xenotransplanted cells by ddPCR: **(A)** TREx-BCBL1-RTA cells reactivated with 1 μg/mL doxycycline in culture and RNA was harvested at latent cells, or cells undergoing lytic replication at 24 or 48 hours post induction (hpi). 500 μM Phosphonoacetic acid (PAA) was used to inhibit replication of the viral genome and late gene expression. qRT-PCR was used to measure transcript abundance of β-actin, the immediate early gene, *RTA*, the early gene, *ORF45* and the late gene *K8.1* (n=4 independent experiments; means ± SEM); **(B)** Western blot of cells treated as in **(A)** and probed for protein expression for the same transcripts; **(C)** ddPCR amplification plot for β-actin, *RTA, ORF45,* and *K8.1*. x-axis displays individual events and y-axis is fluorescent amplitude. For all targets we tested cDNA derived from uninjected larvae, or larvae injected with untreated TREx-BCBL1-*RTA* cells or cells treated with 1 μg/mL doxycycline for 12h prior to injection. RNA was harvested from

larvae at 48 hpi. The pink threshold line separates positive reaction droplets (blue) from negative droplets (grey).

3.4 Engraftment of PEL cells in the yolk sac requires the hypoxic translation initiation factor eIF4E2

The zebrafish yolk sac provides a suitable environment for proliferation of many human cancer cells, including KSHV-infected cells as we have demonstrated (Figure 1 and 2). However, the yolk sac differs from the typical cancer microenvironment because it is acellular, non-vascularized, lacks an extracellular matrix and is rich in lipids [25]; as such, successful proliferation of xenotransplanted cells likely requires metabolic adaptation to this environment. Despite the yolk sac being a common site for xenotransplantation in the zebrafish, surprisingly little is known about what specific pressures a cancer cell encounters in this environment that may affect the interpretation of experiments. Thus, it is important to characterize this microenvironment to better understand the cellular requirements of xenotransplantation and to identify factors, such as oxygen concentration, that could interfere with expected drug activities [26,27]. Although the tissue surrounding the yolk sac is vascularized we hypothesized that the yolk sac itself might be a relatively hypoxic environment as it is unclear how efficiently oxygen penetrates the yolk, also taking into account that site of injection is purposely distant from vasculature as to prevent dissemination of engrafted cells prior to drug treatments. To assess the yolk sac environment, we employed the cell permeable dye Image-iT Green Hypoxia Reagent that only becomes fluorescent at oxygen concentrations below 5% and thus serves as a proxy measure of the oxygen concentration in the zebrafish. Specifically, we labelled TREx-BCBL1-RTA cells with this dye, followed by CMTMR, and injected 2 dpf embryos as described above. We monitored the embryos after injection and within an hour we could observe the appearance of many green fluorescent cells, suggesting they were experiencing a low oxygen environment **(Figure 4A)**.

Given our qualitative results indicating that the yolk sac was potentially a hypoxic environment based on staining with the Image-iT Green Hypoxia Reagent, we sought to determine if the xenografted cells themselves where responding to hypoxia. To address this possibility, we decided to look at the role of the eIF4F complex in xenografted cell proliferation. In normal culture conditions at atmospheric oxygen concentrations, the canonical eIF4F complex is responsible for most translation initiation [28]. During hypoxic conditions of <5% oxygen, eIF4F is disassembled due to mTORC1 inactivation, and the hypoxic eIF4F initiation factor ($eIF4F_H$) assumes a primary role in promoting translation initiation [29]. This complex is activated by the stabilization of hypoxia inducibility factor 2α (HIF-2α) and its subsequent binding to the m^7GTP cap binding protein eIF4E2 [29]. $eIF4F_H$ is required for protein synthesis under hypoxia and subsequently, proliferation of cells within the hypoxic core of a solid tumour in nude mice xenografts or in spheroid culture [29]. Consequently, we hypothesized that xenografts experiencing low oxygen conditions require $eIF4F_H$ activation to proliferate.

To investigate the importance of hypoxic protein synthesis in TREx-BCBL-RTA cells in the zebrafish yolk sac, we silenced eIF4E2 expression by transducing cells with lentiviruses bearing eIF4E2-specific shRNA; lentiviruses bearing a non-targeting shRNA served as a negative control for this experiment. We observed efficient eIF4E2 silencing, with no discernable off-target silencing of the eIF4F component eIF4E1 **(Figure 4B).** In normal cell culture conditions in atmospheric oxygen, there was no difference in proliferation between either the non-targeting shRNA control or the eIF4E2 shRNA compared to parental TREx-BCBL1-RTA cells (**Figure 4C**). However, when these cells were xenotransplanted into the yolk sac, the eIF4E2-silenced cells failed to proliferate as readily as the control cells **(Figure 4D)**. Taken together, these experiments indicate that the zebrafish yolk sac is a functionally hypoxic environment that requires metabolic compensation by the xenografted cells to proliferate.

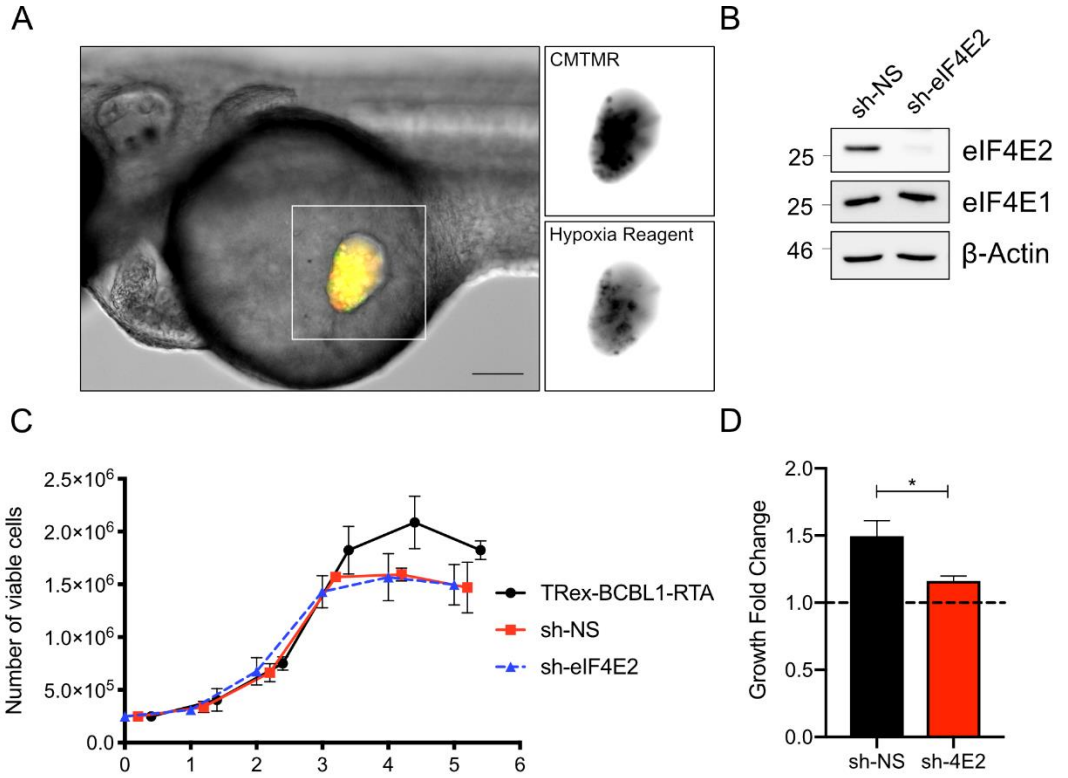

Figure 4. The zebrafish yolk sac is hypoxic and proliferation requires eIF4E2: **(A)** TREx-BCBL1-RTA cells were labelled with 1 μM of Image-iT Green Hypoxia Reagent for 30 min prior to washing and labelling with CMTMR. Cells were injected into 2 dpf embryos and imaged an hour later. Scale bar = 100 μm. **(B)** TREx-BCBL1-RTA cells were transduced with eIF4E2 shRNA or a non-targeting control lentivirus. Cells were harvested and probed for eIF4E2 and homologue eIF4E1 by western blotting; **(C)** TREx-BCBL1-RTA cells or cells transduced as in **(B)** were seeded at 2.5x10^5 cells/mL and monitored for viability and proliferation by manual counting using a hemocytometer and trypan blue for the following 5 days (n= 3 independent transductions; means ±SEM; statistical significance was determined by two way ANOVA); **(D)** Proliferation of transduced TREx-BCBL1-RTA cells at 3 dpi normalized to the number of cells counted at 1 dpi (n= 3 independent experiments with cells from 20 larvae counted per measurement; means ± SEM; statistical significance was determined by two-way ANOVA compared to the cell counts at 1 dpf).

4. Discussion

Zebrafish have been used to model a variety of hematopatholocial malignancies [9]. Because zebrafish exclusively rely on innate immunity until adaptive immunity develops at approximately 28 dpf, human cells can engraft and proliferate without the need for immunosuppression [10]. Building upon our expertise with zebrafish XT models of leukemias and lymphomas, we developed the first *in vivo* model for a virally-induced lymphoma in zebrafish. We demonstrated that KSHV-infected PEL cells readily proliferate in the embryo yolk sac. The embryos tolerate xenotransplantation of the cells, with survival rates comparable to controls. We took advantage of the well-established paradigm of KSHV latency and lytic replication to determine if we could successfully activate a Tet-regulated cassette in a xenograft by adding doxycycline directly to the fish water. While we were able to demonstrate activation of Tet-driven *RTA* expression by monitoring RFP expression in xenografted iSLK.219 cells, this was relatively inefficient. However, these experiments suggest that Tet-regulated promoters in xenotransplanted cells can respond to doxycycline in the fish water, which may be useful in other studies requiring stimulating gene expression post-XT.

Zebrafish xenografts have been typically evaluated by measuring XT cell proliferation and migration into other tissues, and determining whether exogenous chemicals can impact these processes[12]. There are few studies of gene expression in the xenografted cells as there are so few transplanted cells compared to the zebrafish cells that XT transcripts cannot be easily detected at a quantitative threshold using qRT-PCR [30]. In this study, we developed sensitive new methods to detect viral and host gene expression in xenotransplants using ddPCR. The ease and sensitivity of ddPCR technology suggests that it may also be adapted to replace current laborious microscopy-based methods for monitoring xenograft cell proliferation. The relatively low quantity of XT human transcripts compared to abundant larval host transcripts has made it difficult to quantify differences in abundance of XT transcripts. This limitation can be surmounted by probing abundant Alu repeat retroelements by QPCR; there are approximately 10^6 Alu copies per human genome [31]. While preparing this article, Salo and colleagues (2019) also demonstrated the use of RT-qPCR to monitor XT proliferation by targeting the abundant glyceraldehyde-3-phosphate dehydrogenase (GAPDH) transcript [30]. They also demonstrated that less abundant cytokeratin 17 transcript could be detected by ddPCR and that the number of detected copies/μL tightly correlated with the size of the XT as determined by both fluorescent quantification and qPCR for GAPDH [30]. We suspect that the sensitivity of ddPCR is likely sufficient to directly quantify XT load by detection of XT DNA. Nevertheless, we maintain that the primary application of ddPCR technology in zebrafish XT models will likely be gene expression analysis of XTs in response to drug treatments or changes in the XT microenvironment.

We took advantage of the well-developed Tet-regulated induction of the KSHV lytic cycle to determine if we could stimulate gene expression in the xenograft and if we could detect viral gene expression using the specific and highly-sensitive ddPCR platform. We successfully detected mRNA from all temporal classes of gene expression including some lytic gene expression in untreated cells. KSHV latency is unstable in culture and lytic gene expression can be detected in a small percentage of cells (<1%). Accordingly, the presence of lytic gene products in these xenografts could reflect normal rates of spontaneous lytic replication. However, we think it is more likely that the hypoxic microenvironment of the XT may stimulate transcription of the KSHV lytic switch protein RTA, as has been reported in previous *in vitro* studies [32]. Even though we could detect KSHV lytic gene products in the xenograft, it remains unclear whether this is sufficient to support production of infectious virions *in situ*, which will require further development of sensitive detection methods. Studies of human viral replication in zebrafish can be confounded by the normal maintainence temperature of zebrafish (28°C), which is lower then typical human cell culture conditions (37°C) [15]. This temperature gap is largely overcome in our xenotransplantation model where the larvae are housed at 35°C, which is likely to be permissive for KSHV replication. Anecdotally, we did not notice any GFP+ cells distal to the XT injection site that could indicate dissemination of xenografted human cells or KSHV infection of zebrafish larval cells.

In this study, we did not attempt to directly infect the zebrafish embryos or zebrafish cell lines with KSHV. However, there have been reports of direct infection of adult zebrafish with the human alphaherpesvirus herpes simplex virus type 1 (HSV-1) by intraperitoneal injection [33]. HSV-1 replicates in the fish at 28°C and replication could be inhibited with the herpesvirus antiviral acyclovir. Viral antigens could be detected in the nervous tissue, an important site of HSV-1 latency and pathogenesis, suggesting the potential of zebrafish to model viral encephalitis [33]. However, since KSHV is highly restricted to primates and cannot productively infect other mammals, including mice [34], we reasoned that zebrafish cells would be unlikely to support KSHV replication.

The zebrafish XT model provides a convenient low-cost model to study interactions of xenotransplanted cancer cells, including KSHV-infected PEL cells, with a complex 3D microenvironment. Further study of the properties of this microenvironment will inform our understanding of the potential metabolic compensation required for cancer cells to proliferate in this niche. A recent study conducted by our group suggested that the yolk sac likely does not provide the

same extracellular matrix context present in a solid tumor. As a result of this microenvironment feature, resistance to anoikis, a mode of programmed cell death initiated after loss of contract with the extracellular matrix, is required to support increased XT proliferation in this compartment [26]. Our experiments with a hypoxia-responsive dye suggests that xenografts likely also experience a hypoxic environment in the yolk sac, with an oxygen tension likely below normal tissue "physoxia" of 5%, and more similar to many solid tumors [35,36]. We demonstrate that this environment required specific metabolic compensation by the xenograft in activation of the eIF4E2-dependent eIF4F$_H$ translation initiation complex. Hypoxia drives significant changes in both the transcriptome and the proteome. However, most of the changes to the proteome are derived from a global reprogramming of the translational efficiencies of mRNA rather than changes to the transcriptome [37]. The hypoxic state of the yolk sac should be considered when modelling human cancers in zebrafish embryos [36].

Hypoxia can influence the proliferation and migration of cancer cells, partially as a result of the influence of oxygen concentration and hypoxia inducible factors on angiogenesis [38]. Furthermore, the responses of cancer cells to multiple drugs can be altered in hypoxic conditions. For example, hypoxia can induce resistance to cisplatin treatment in multiple cancer types [39]. This is an important factor to consider when designing zebrafish XT experiments targeting the yolk sac, especially in a drug screening schema, where the effects of compounds may be masked or amplified as a result of low oxygen levels. Embryos can tolerate xenotransplantation in other anatomical sites such as the circulation, the hindbrain ventricle, or the perivitelline space, which should be considered as injection sites, along with the yolk sack, when designing XT studies [9].

In summary, we present a novel zebrafish xenograft model for PEL that is a convenient low-cost alternative to existing murine models that obviates the need for potentially confounding immunosuppressive treatments. This model could serve as an excellent platform for *in vivo* patient derived xenograft (PDX) experiments, akin to those done by others [40]. However, unlike those experiments in murine models, or in immune-deficient adult zebrafish models [41], these experiments only require small numbers of cells, conserving this rare primary patient material. Nonetheless, it is important to note that these larval experiments will not replace murine or adult zebrafish xenograft models; rather, it is our hope that this model can supplement the battery of techniques already available to study PEL and other viral cancers *in vivo*.

Author Contributions: conceptualization, E.S.P., J.W., G.D., J.N.B., and C.M.; methodology, E.S.P., J.W., N.M., A.L.Y., C.V., M.N.H., T.D.; investigation, E.S.P., J.W., N.M., A.J.C., A.L.Y., C.V., C.-A.R., M.N.H.; writing—original draft preparation, E.S.P., J.W., J.N.B., C.M.; writing—review and editing, all authors; supervision, T.D., J.N.B., C.M.; funding acquisition, G.D., T.D., J.N.B., C.M.

Funding: E.S.P. was supported by a trainee award from the Beatrice Hunter Cancer Research Institute with funds provided by the Canadian Imperial Bank of Commerce as part of The Terry Fox Strategic Health Research Training Program in Cancer Research at CIHR. J.W. was supported by an IWK Health Center Graduate Scholarship. This work was supported by Nova Scotia Health Research Foundation Development/Innovative Grant MED-Capacity-2012-8464, Canadian Breast Cancer Foundation (CBCF) – Atlantic Chapter - Research Grant 14787 and Canadian Institutes for Health Research Operating Grant MOP-84554.

Acknowledgments: We thank Gretchen Wagner, David Malloy, and the Dalhousie Zebrafish CORE facility for animal husbandry and members of the Berman and McCormick laboratories for helpful discussions. Reagents were generously provided by Don Ganem (UCSF; Chan-Zuckerberg Biohub), David Lukac (Rutgers), Jae Jung (USC), and Didier Trono (EPFL).

Conflicts of Interest: The authors declare no conflict of interest. The funders had no role in the design of the study; in the collection, analyses, or interpretation of data; in the writing of the manuscript, or in the decision to publish the results.

References

1. Soulier, J.; Grollet, L.; Oksenhendler, E.; Cacoub, P.; Cazals-Hatem, D.; Babinet, P.; d'Agay, M. F.; Clauvel, J. P.; Raphael, M.; Degos, L. Kaposi's sarcoma-associated herpesvirus-like DNA sequences in multicentric Castleman's disease. *Blood* **1995**, *86*, 1276–1280.
2. Hassman, L. M.; Ellison, T. J.; Kedes, D. H. KSHV infects a subset of human tonsillar B cells, driving proliferation and plasmablast differentiation. *JCI.* **2011**, *121*, 752–768.
3. Grundhoff, A.; Ganem, D. Inefficient establishment of KSHV latency suggests an additional role for continued lytic replication in Kaposi sarcoma pathogenesis. *JCI* **2004**, *113*, 124–136.
4. Simonelli, C.; Spina, M.; Cinelli, R.; Talamini, R.; Tedeschi, R.; Gloghini, A.; Vaccher, E.; Carbone, A.; Tirelli, U. Clinical features and outcome of primary effusion lymphoma in HIV-infected patients: a single-institution study. *JCO* **2003**, *21*, 3948–3954.
5. Arora, N.; Gupta, A.; Sadeghi, N. Primary effusion lymphoma. *Curr Opin Pulm Med* **2017**, *23*, 365–370.
6. Staudt, M. R.; Kanan, Y.; Jeong, J. H.; Papin, J. F.; Hines-Boykin, R.; Dittmer, D. P. The tumor microenvironment controls primary effusion lymphoma growth in vivo. *Cancer Res* **2004**, *64*, 4790–4799.
7. Caro-Vegas, C.; Bailey, A.; Bigi, R.; Damania, B.; Dittmer, D. P. targeting mTOR with MLN0128 overcomes rapamycin and chemoresistant primary effusion lymphoma. *mBio* **2019**, *10*.
8. Martin, D.; Nguyen, Q.; Molinolo, A.; Gutkind, J. S. Accumulation of dephosphorylated 4EBP after mTOR inhibition with rapamycin is sufficient to disrupt paracrine transformation by the KSHV vGPCR oncogene. *Oncogene* **2013**, 1–8.
9. Wertman, J.; Veinotte, C. J.; Dellaire, G.; Berman, J. N. The zebrafish xenograft platform: evolution of a novel cancer model and preclinical screening tool. In *Adv Exp Med*; Advances in Experimental Medicine and Biology; Springer International Publishing: Cham, 2016; Vol. 916, pp. 289–314.
10. Lam, S. H.; Chua, H. L.; Gong, Z.; Lam, T. J.; Sin, Y. M. Development and maturation of the immune system in zebrafish, Danio rerio: a gene expression profiling, in situ hybridization and immunological study. *Dev Comp* **2004**, *28*, 9–28.
11. Amatruda, J. F.; Zon, L. I. Dissecting hematopoiesis and disease using the zebrafish. *Dev Biol* **1999**, *216*, 1–15.
12. Corkery, D. P.; Dellaire, G.; Berman, J. N. Leukaemia xenotransplantation in zebrafish--chemotherapy response assay in vivo. *Br J Haematol* **2011**, *153*, 786–789.
13. Bentley, V. L.; Veinotte, C. J.; Corkery, D. P.; Pinder, J. B.; LeBlanc, M. A.; Bedard, K.; Weng, A. P.; Berman, J. N.; Dellaire, G. Focused chemical genomics using zebrafish xenotransplantation as a pre-clinical therapeutic platform for T-cell acute lymphoblastic leukemia. *Haematologica* **2014**, *100*, 70–76.
14. White, R. M.; Sessa, A.; Burke, C.; Bowman, T.; LeBlanc, J.; Ceol, C.; Bourque, C.; Dovey, M.; Goessling, W.; Burns, C. E.; Zon, L. I. Transparent adult zebrafish as a tool for in vivo transplantation analysis. *Cell Stem Cell* **2008**, *2*, 183–189.
15. Westerfield, M. *The zebrafish book. a guide for the laboratory use of zebrafish (Danio rerio)*; 5 ed.; University of Oregon Press: Eugene, **2007**.
16. Renne, R.; Zhong, W.; Herndier, B.; Ganem, D. Lytic growth of Kaposi's sarcoma-associated herpesvirus (human herpesvirus 8) in culture. *Nat Med* **1996**, *2*, 342–346.
17. Nakamura, H.; Lu, M.; Gwack, Y.; Souvlis, J.; Zeichner, S. L.; Jung, J. U. Global changes in Kaposi's sarcoma-associated virus gene expression patterns following expression of a tetracycline-inducible Rta transactivator. *J Virol* **2003**, *77*, 4205–4220.
18. Stürzl, M.; Gaus, D.; Dirks, W. G.; Ganem, D.; Jochmann, R. Kaposi's sarcoma-derived cell line SLK is not of endothelial origin, but is a contaminant from a known renal carcinoma cell line. *Int J Cancer* **2012**, *132*:1954-8. doi: 10.1002/ijc.27849.
19. Vieira, J.; O'Hearn, P. M. Use of the red fluorescent protein as a marker of Kaposi's sarcoma-associated herpesvirus lytic gene expression. *Virology* **2004**, *325*, 225–240.
20. Myoung, J.; Ganem, D. Generation of a doxycycline-inducible KSHV producer cell line of endothelial origin: maintenance of tight latency with efficient reactivation upon induction. *J Virol* **2011**, *174*, 12–21.
21. Carpenter, A. E.; Jones, T. R.; Lamprecht, M. R.; Clarke, C.; Kang, I. H.; Friman, O.; Guertin, D. A.; Chang, J. H.; Lindquist, R. A.; Moffat, J.; Golland, P.; Sabatini, D. M. CellProfiler: image analysis software for identifying and quantifying cell phenotypes. *Genome Biol* **2006**, *7*, R100.
22. Bechtel, J. T.; Liang, Y.; Hvidding, J.; Ganem, D. Host range of Kaposi's Sarcoma-Associated Herpesvirus in cultured cells. *J Virol* **2003**, *77*, 6474–6481.

23. Hindson, B. J.; Ness, K. D.; Masquelier, D. A.; Belgrader, P.; Heredia, N. J.; Makarewicz, A. J.; Bright, I. J.; Lucero, M. Y.; Hiddessen, A. L.; Legler, T. C.; Kitano, T. K.; Hodel, M. R.; Petersen, J. F.; Wyatt, P. W.; Steenblock, E. R.; Shah, P. H.; Bousse, L. J.; Troup, C. B.; Mellen, J. C.; Wittmann, D. K.; Erndt, N. G.; Cauley, T. H.; Koehler, R. T.; So, A. P.; Dube, S.; Rose, K. A.; Montesclaros, L.; Wang, S.; Stumbo, D. P.; Hodges, S. P.; Romine, S.; Milanovich, F. P.; White, H. E.; Regan, J. F.; Karlin-Neumann, G. A.; Hindson, C. M.; Saxonov, S.; Colston, B. W. High-throughput droplet digital pcr system for absolute quantitation of dna copy number. *Anal Chem* **2011**, *83*, 8604–8610.
24. Overby, L. R.; Robishaw, E. E.; Schleicher, J. B.; Rueter, A.; Shipkowitz, N. L.; Mao, J. C. Inhibition of herpes simplex virus replication by phosphonoacetic acid. *Antimicrob Agents Chemother* **1974**, *6*, 360–365.
25. Fraher, D.; Sanigorski, A.; Mellett, N. A.; Meikle, P. J.; Sinclair, A. J.; Gibert, Y. Zebrafish embryonic lipidomic analysis reveals that the yolk cell is metabolically active in processing lipid. *Cell Reports* **2016**, *14*, 1317–1329.
26. Corkery, D. P.; Clarke, L. E.; Gebremeskel, S.; Salsman, J.; Pinder, J.; Le Page, C.; Meunier, L.; Xu, Z.; Mes-Masson, A.-M.; Berman, J. N.; Johnston, B.; Dellaire, G. Loss of PRP4K drives anoikis resistance in part by dysregulation of epidermal growth factor receptor endosomal trafficking. *Oncogene* **2017**, *37*, 174–184.
27. Strese, S.; Fryknäs, M.; Larsson, R.; Gullbo, J. Effects of hypoxia on human cancer cell line chemosensitivity. *BMC Cancer* **2013**, *13*, 331.
28. Thoreen, C. C.; Chantranupong, L.; Keys, H. R.; Wang, T.; Gray, N. S.; Sabatini, D. M. A unifying model for mTORC1-mediated regulation of mRNA translation. *Nature* **2012**, *486*, 109–113.
29. Uniacke, J.; Holterman, C. E.; Lachance, G.; Franovic, A.; Jacob, M. D.; Fabian, M. R.; Payette, J.; Holcik, M.; Pause, A.; Lee, S. An oxygen-regulated switch in the protein synthesis machinery. *Nature* **2013**, *486*, 126–129.
30. Al-Samadi, A.; Tuomainen, K.; Kivimäki, A.; Salem, A.; Al-Kubati, S.; Hyytiäinen, A.; Parikka, M.; Mesimäki, K.; Wilkman, T.; Mäkitie, A.; Grenman, R.; Salo, T. PCR-based zebrafish model for personalised medicine in head and neck cancer. *J transl Med* **2019**, 1–6.
31. Haque, M.; Davis, D. A.; Wang, V.; Widmer, I.; Yarchoan, R. Kaposi's Sarcoma-Associated Herpesvirus (Human Herpesvirus 8) contains hypoxia response elements: relevance to lytic induction by hypoxia. *J Virol* **2003**, *77*, 6761–6768.
32. Burgos, J. S.; Ripoll-Gomez, J.; Alfaro, J. M.; Sastre, I.; Valdivieso, F. Zebrafish as a new model for herpes simplex virus type 1 infection. *Zebrafish* **2008**, *5*, 323–333.
33. Austgen, K.; Oakes, S. A.; Ganem, D. Multiple Defects, Including Premature Apoptosis, Prevent Kaposi's Sarcoma-Associated Herpesvirus Replication in Murine Cells. *Journal of Virology* **2012**, *86*, 1877–1882.
34. Batzer, M. A.; Deininger, P. L. Alu repeats and human genomic diversity. *Nat Rev Genet* **2002**, *3*, 370–379.
35. McKeown, S. R. Defining normoxia, physoxia and hypoxia in tumours—implications for treatment response. *BJR* **2014**, *87*, 20130676.
36. Uniacke, J.; Kishan Perera, J.; Lachance, G.; Francisco, C. B.; Lee, S. Cancer Cells Exploit eIF4E2-Directed Synthesis of Hypoxia Response Proteins to Drive Tumor Progression. *Cancer Res* **2014**.
37. Ho, J. J. D.; Wang, M.; Audas, T. E.; Kwon, D.; Carlsson, S. K.; Timpano, S.; Evagelou, S. L.; Brothers, S.; Gonzalgo, M. L.; Krieger, J. R.; Chen, S.; Uniacke, J.; Lee, S. Systemic reprogramming of translation efficiencies on oxygen stimulus. *Cell Reports* **2016**, *14*, 1293–1300.
38. Hirota, K.; Semenza, G. L. Regulation of angiogenesis by hypoxia-inducible factor 1. *CRC Cr Rev Oncol-Hemat* **2006**, *59*, 15–26.
39. Wohlkoenig, C.; Leithner, K.; Deutsch, A.; Hrzenjak, A.; Olschewski, A.; Olschewski, H. Hypoxia-induced cisplatin resistance is reversible and growth rate independent in lung cancer cells. *Cancer Lett* **2011**, *308*, 134–143.
40. Sarosiek, K. A.; Cavallin, L. E.; Bhatt, S.; Toomey, N. L.; Natkunam, Y.; Blasini, W.; Gentles, A. J.; Ramos, J. C.; Mesri, E. A.; Lossos, I. S. Efficacy of bortezomib in a direct xenograft model of primary effusion lymphoma. *P Natl Acad Sci USA* **2010**, *107*, 13069–13074.
41. Yan, C.; Brunson, D. C.; Tang, Q.; Do, D.; Iftimia, N. A.; Moore, J. C.; Hayes, M. N.; Welker, A. M.; Garcia, E. G.; Dubash, T. D.; Hong, X.; Drapkin, B. J.; Myers, D. T.; Phat, S.; Volorio, A.; Marvin, D. L.; Ligorio, M.; Dershowitz, L.; McCarthy, K. M.; Karabacak, M. N.; Fletcher, J. A.; Sgroi, D. C.; Iafrate, J. A.; Maheswaran, S.; Dyson, N. J.; Haber, D. A.; Rawls, J. F.; Langenau, D. M. Visualizing engrafted human cancer and therapy responses in immunodeficient zebrafish. *Cell* **2019**, *177*, 1903–1914.e14.